

Seychelles Plateau's oil spill vulnerability

Alex Verhofstede^a, Thomas Dobbelaere^a, Jérôme Harlay^b, Emmanuel Hanert^{a,c}

^a *Earth and Life Institute (ELI), UCLouvain, Louvain-la-Neuve, Belgium*

^b *Blue Economy Research Institute (BERI), University of Seychelles, Mahé, Seychelles*

^c *Institute of Mechanics, Materials and Civil Engineering (IMMC), UCLouvain, Louvain-la-Neuve, Belgium*

Abstract

Small Island Developing States, such as Seychelles, are highly susceptible to oil pollution incidents, with limited infrastructure for detection and mitigation. While an oil spill could significantly impact Seychelle's tourism industry, contributing to ~40% of its GDP, the archipelago's vulnerability remains largely unknown. Here, we developed a high-resolution ocean circulation model for Seychelles Plateau, simulating currents over three years (2018-2020) to model oil spill dispersal to six ecologically and economically significant coastal areas. Our findings reveal distinct seasonality in offshore risk distribution, driven by seasonal fluctuations in atmospheric and oceanic circulations. We show that an oil spill originating from any part of the plateau could potentially impact a sensitive coastal site in less than five days. By identifying high-risk areas, including the major north-south shipping route, we emphasize the importance of close satellite and airborne monitoring for early warnings to protect Seychelles' coastal ecosystems and tourism industry.

Keywords: Seychelles Plateau, multiscale coastal ocean model, oil spill risk, backtracking

Email address: emmanuel.hanert@uclouvain.be (Emmanuel Hanert)

1 **1. Introduction**

2 Small Island Developing States (SIDS) are a unique group of nations that face
3 distinct challenges due to their geographical, socio-economic, and environmental
4 characteristics (Nurse et al., 2014). Comprising small land areas and isolated loca-
5 tions, SIDS are particularly susceptible to a wide range of vulnerabilities, includ-
6 ing climate change, natural disasters, and limited resource availability (Betzold,
7 2015). Among these challenges, their heightened vulnerability to oil spills has
8 emerged as a pressing concern with potential long-lasting consequences (Farbotko
9 and Lazrus, 2012). Oil spills pose significant risks to SIDS, as their economies
10 largely depend on coastal resources, particularly tourism and fisheries (Briguglio,
11 1995). Given the interconnectedness of marine ecosystems, oil spills can lead to
12 the deterioration of coral reefs, mangroves, and seagrass beds, directly impact-
13 ing the livelihoods of local communities (Nurse et al., 2014). Additionally, the
14 tourism industry, which often serves as the economic backbone of these island
15 states, can be severely affected by oil spills, resulting in reduced tourist arrivals
16 and loss of revenue (Scheyvens and Momsen, 2008).

17 Due to their small size and limited resources, SIDS often lack the infrastruc-
18 ture and capacity to effectively respond to oil spills, further exacerbating the im-
19 pacts on local ecosystems and economies (Campbell and Barnett, 2010). Strength-
20 ening their preparedness and response capabilities is crucial in order to mitigate
21 the risks associated with oil spills. This may include the implementation of early
22 warning systems, enhancement of regional collaboration, and the development of
23 robust contingency plans (Farbotko and Lazrus, 2012). Addressing this challenge
24 is essential for the sustainable development and resilience of SIDS in the face of

25 growing environmental threats (Nurse et al., 2014).

26 Seychelles, an archipelago in the Indian Ocean, is a typical example of a SIDS
27 particularly vulnerable to oil spills (Campling and Rosalie, 2006). With tourism
28 accounting for 42% of its gross domestic product (GDP) in 2019 (World Travel &
29 Tourism Council, 2022). Seychelles' economy could be severely impacted by an
30 oil spill. Although recent minor oil spills have been manageable through disper-
31 sant spraying (ITOPF, 2005), the country experienced a major incident in 1970
32 when the British tanker Ennerdale, carrying 41,500 tons of oil products, sank off
33 the coast of Mahé (The New York Times, 1970). Another notable event occurred
34 in 2020, when the MV Wakashio bulk carrier ran aground in Mauritius, result-
35 ing in the leakage of approximately 1000 tons of oil into the surrounding waters
36 (Gurumoorthi et al., 2021). While not directly threatening Seychelles, this inci-
37 dent highlighted the vulnerability of Mauritius, a SIDS just south of Seychelles,
38 to maritime pollution and the subsequent ecological and economic impacts.

39 While Seychelles has developed an oil spill mitigation strategy, which includes
40 the Seychelles National Oil Spill Contingency Plan (NOSCP) to enhance pre-
41 paredness and response capabilities (Government of Seychelles, 2018). There are
42 several limitations that may hinder the effectiveness of these efforts. As a SIDS,
43 Seychelles faces resource constraints in terms of financial, human, and techno-
44 logical capacity (Briguglio, 1995; Campling and Rosalie, 2006). This may affect
45 its ability to invest in state-of-the-art equipment, infrastructure, and training re-
46 quired to efficiently manage and respond to oil spills. The archipelago's remote
47 location also poses logistical challenges in accessing international support, re-
48 sources, and expertise during an oil spill incident (Farbotko and Lazrus, 2012).
49 Finally, the comprehensive monitoring of maritime traffic and potential oil spill

50 risks over a large sea area is very resource-intensive. Seychelles hence lacks the
51 necessary infrastructure or technology, such as satellite and airborne synthetic-
52 aperture radar, to continuously monitor its vast exclusive economic zone (EEZ)
53 for potential threats.

54 The aim of this study is to enhance Seychelles' oil spill preparedness by pin-
55 pointing offshore regions posing the greatest risk to coastal areas of significant
56 ecological or economic value in the event of an oil spill. To accomplish this, we
57 employ a high-resolution ocean model to simulate ocean circulation over the Sey-
58 chelles Plateau (SP) and utilize the generated currents to model oil spill dispersal
59 across three consecutive years (2018-2020). The oil dispersal simulations produce
60 monthly oil spill risk estimates, which are then integrated with shipping lanes and
61 oil extraction maps for the SP to identify pollution exposure hotspots related to
62 these activities. We recommend prioritizing monitoring resources in these identi-
63 fied areas.

64 **2. Material and methods**

65 To assess the vulnerability of Seychelles' coastal assets to oil spills, we sim-
66 ulate the dispersal of oil particles backward in time, starting from some selected
67 sensitive coastal areas on SP. These simulations allow us to identify offshore ar-
68 eas from where an oil spill would have a high probability of reaching one of those
69 sensitive areas, and to estimate the time needed for the spill to reach that area.
70 The subsequent sections provides a detailed explanation of our methodology, be-
71 ginning with a description of the study area.

72 *2.1. Study area*

73 The Seychelles archipelago is situated approximately 1200 km northeast of
74 Madagascar in the western Indian Ocean (Fig. 1a). Comprising 115 islands that
75 cover around 455 km² of land, only a third of them are inhabited (Podhorodecka,
76 2018). The nation's population of about 87,000 residents (McEwen and Bennett,
77 2010) primarily reside on the three main islands: Mahé, Praslin, and La Digue.
78 These islands, along with others in the archipelago, are situated on the Mahé or
79 Seychelles Plateau (SP, Fig. 1b), spanning approximately 40,000 km² (Seychelles
80 Fishing Authority, 2019) and extending around 350 km latitudinally and 150 km
81 meridionally (Castillo-Trujillo et al., 2021). The relatively shallow plateau, with
82 an average depth of about 50 m, plunges to depths exceeding 2000 m at its edges
83 (Castillo-Trujillo et al., 2021). The Seychelles archipelago holds significant eco-
84 logical value. Due to its geographic isolation, the islands foster high levels of
85 endemism. It is estimated that between 50 and 80% of animal species and 45% of
86 plant species are endemic. Rocamora and Skerrett (2001) list 11 bird species that
87 are endemic to Seychelles. Additionally, the coral reefs surrounding much of the
88 Seychelles serve as habitats for numerous fish species (Techera, 2019).

89 Maritime traffic in the Seychelles primarily follows a North-South naviga-
90 tion axis across the SP (Fig. 1c). This axis leads through the port of Victo-
91 ria, the archipelago's main port and point of entry for 95% of the country's im-
92 ports (Agence Française de Développement, 2018). Ships navigate around the
93 northeastern side of Mahé Island, potentially making this area more suscepti-
94 ble to oil spills (MarineTraffic, 2023). Additionally, there is shipping between
95 Mahé, Praslin, and La Digue islands, as passenger transport catamarans connect
96 them. Though Victoria is the primary port, its limited capacity often necessitates

97 berthing boats at the entrance. Currently, there is no active oil extraction on the SP.
98 However, two areas within the plateau are under petroleum exploration licenses,
99 and several wells have been drilled in the past, posing a risk of oil leakage on
100 the plateau (Fig. 1d, PetroSeychelles, 2023). Moreover, the Cabinet of Ministers
101 has approved a new petroleum exploration contract in the SP's southeast region
102 (Zabasajja and Bhuckory, 2022).

103 For this study, we assessed the oil spill vulnerability of six coastal areas on
104 SP that have a particularly high ecological and economic value (Fig. 1b). They
105 include Seychelles' main marine national parks (MNP's) and protected areas such
106 as Saint Anne MNP located east of Mahé, Port Launay and Baie Ternay on the
107 northwest coast of Mahé, Silhouette MNP, Curieuse MNP, Denis Island and Bird
108 Island. These protected areas play a crucial role in conserving the Seychelles' rich
109 marine biodiversity and promoting sustainable tourism. We also considered the
110 touristic islands of Praslin and La Digue, as well as the port of Victoria that plays
111 a crucial role in Seychelles' economy as it is the main gateway for international
112 trade, handling the majority of cargo traffic in and out of the country. It serves as a
113 base for the country's fishing fleet and as a point of entry for cruise ships, yachts,
114 and other vessels carrying tourists.

115 2.2. *Oil dispersal model*

116 We simulate oil spill dispersal using the open-source OpenOil model, devel-
117 oped by the Norwegian Meteorological Institute (Röhrs et al., 2018; Dagestad
118 et al., 2017). OpenOil is a Lagrangian model that represents oil spills as ensem-
119 bles of oil particles. The horizontal transport of oil particles is influenced by
120 three processes: (1) ocean currents, (2) surface wind-generated waves through the
121 Stokes drift, which is equal to 1.5% of the wind velocity at the surface and de-

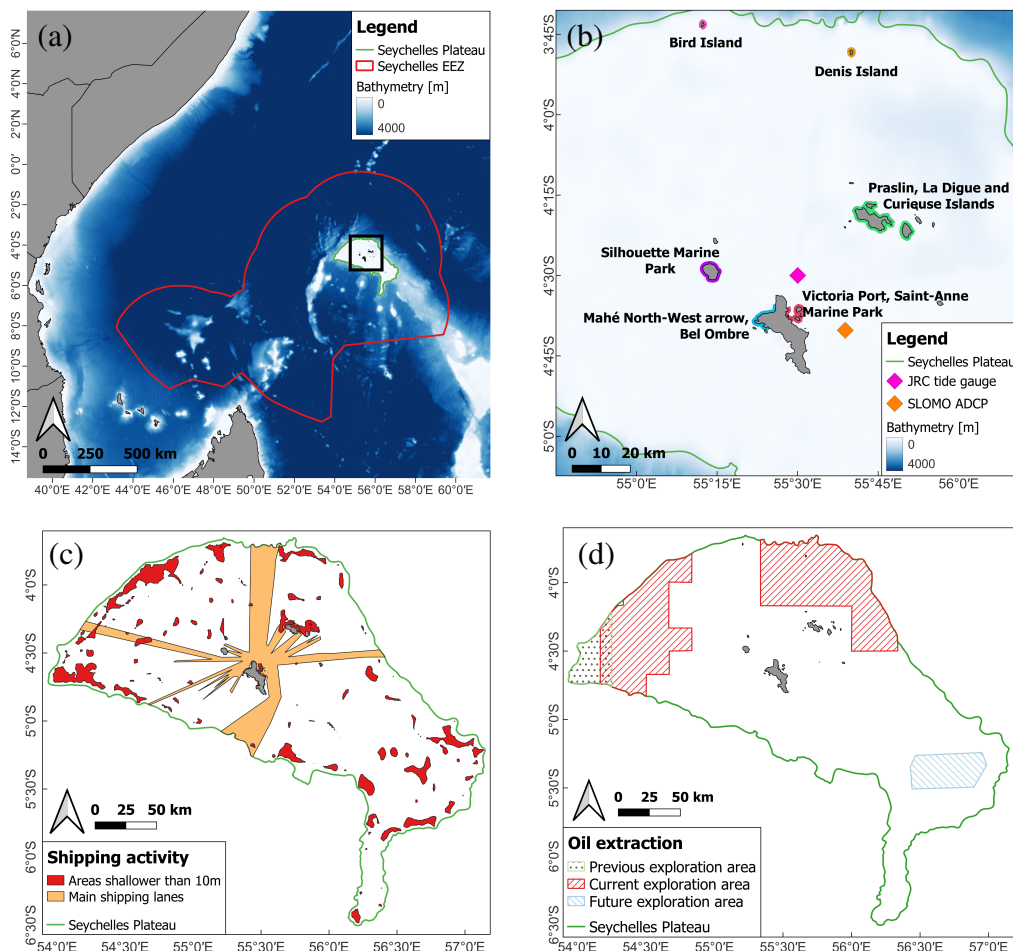


Figure 1: Overview of the area of interest with (a) the extent of Seychelles EEZ in the Indian Ocean, the bathymetry and the location of Seychelles Plateau (SP), (b) close-up view on SP corresponding to the black box in panel (a) with the locations of the 6 sensitive coastal areas, (c) the location of the main shipping lanes and accident-prone areas and (d) the location of past, present and future oil extraction areas.

122 creases with depth (Ardhuin et al., 2009; Jones et al., 2016; Breivik et al., 2016),
123 and (3) wind, causing an additional surface velocity equal to 2% of the wind
124 velocity. The oil spill vertical dynamics is influenced by several factors. First,
125 breaking waves can entrain surface oil particles beneath the ocean surface (Jones
126 et al., 2016). Second, oil particle buoyancy depends on oil viscosity, oil density,
127 seawater temperature, salinity, and oil droplet size distribution (Tkalic and Chan,
128 2002). Finally, oil particles within the water column are subject to vertical turbu-
129 lence, which depends on ocean stratification and shear stress. OpenOil accounts
130 for these physical processes, which have been thoroughly parametrized and val-
131 idated in multiple studies (Röhrs et al., 2018; Dagestad et al., 2017; Jones et al.,
132 2016).

133 Oil spill transport simulations can be conducted forward and backward in time.
134 The forward approach simulates the future movement of a spill from its release
135 point to its final destination, estimating the area that will be affected by an oil spill
136 from a specific location and time. This approach is typically used for operational
137 forecasting and contingency planning (Zodiatis et al., 2016). In contrast, the back-
138 ward approach simulates the spill's past evolution, starting from its final destina-
139 tion and moving backward in time to estimate the spill's origin (Batchelder, 2006).
140 This method is most efficient when the impacted area is known but the pollution
141 source remains unidentified. However, the backward approach does not consider
142 oil weathering processes, which cause changes in the oil's chemical composition
143 and physical characteristics. Consequently, the oil type has limited impact on the
144 results, influencing only the vertical dynamics of oil particles through droplet size
145 distribution, density, and viscosity. As Ciappa (2021) and Anselain et al. (2023),
146 we set the duration for each backward simulation to 5 days. Within this timeframe,

147 the oil spill can typically travel a distance greater than the distance between the
148 selected sensitive coastal areas and the boundaries of the SP, where our model is
149 applied. The uncertainty regarding the spill's position increases with the duration
150 of the simulation, due to both the diffusivity incorporated in OpenOil (set here to
151 $2 \text{ m}^2/\text{s}$) to account for subgrid-scale processes, and the uncertainties in the oceanic
152 and atmospheric forcings. Consequently, a 5-day duration has been chosen as an
153 optimal balance between the accuracy and practicality of our results.

154 As the aim of this study is to assess the vulnerability of Seychelles' main
155 coastal assets to oil spills, the backward approach is most suitable. We considered
156 a distillate marine fuel of 35° API as this type of fuel is now steadily replacing
157 the higher-viscosity and higher-sulfur heavy fuels that used to the standard ship-
158 ping fuels. By choosing this type of fuel, we implicitly assume that the most
159 likely source of pollution are shipping accidents and shipping operations such as
160 ballast cleaning. Default values were used for droplet size and entrainment rate
161 (Dagestad et al., 2017). Obviously, distillate oil is not representative of the crude
162 oil extracted on SP. The precise oil type used in the simulation has however a
163 limited impact on the backward oil spill modelling results, as it only influences
164 the vertical oil distribution and not the oil weathering processes. We conducted a
165 sensitivity analysis with other oil types and found very similar results. To initiate
166 the backward simulations, oil particles were released from receptor points located
167 0.004° ($\approx 400 \text{ m}$) away from the sensitive coastal areas and separated by 0.002°
168 ($\approx 200 \text{ m}$). The number of receptor points per coastal area depends on the length
169 of the coastline. Bird and Denis Islands have the shortest coastline and hence
170 the smallest number of receptor points (resp. 21 and 22). Praslin, La Digue and
171 Curieuse Islands have together the longest coastline, which is represented by 228

172 receptor points. We released 15 oil particles from each receptor point every day
173 of the 2018-2020 period at midnight. During the 3-year period, the transport of
174 $\sim 7.79 \times 10^6$ particles was simulated.

175 The ocean currents that drive oil spill dispersal are simulated using the multi-
176 scale ocean model SLIM¹. SLIM solves the ocean circulation governing equations
177 on an unstructured mesh, which allows for locally increased resolution to accu-
178 rately capture variations in bathymetry and coastal topography. In this study, we
179 focus on simulating the ocean circulation solely on the SP. Given its relatively
180 shallow average depth of 50 m (Castillo-Trujillo et al., 2021), we employ the 2D
181 barotropic version of SLIM. For the same computational cost, a 2D model can
182 achieve a considerably higher horizontal resolution compared to a 3D model. In
183 shallow areas like the SP, small-scale horizontal features are anticipated to have
184 a more significant influence on large-scale oil dispersal patterns than vertical dy-
185 namics. The model mesh has a horizontal resolution reaching about 200 m along
186 all the islands' coastlines on the SP. The resolution coarsens to about 4 km off-
187 shore. The model bathymetry is a combination of the GEBCO (General Bathy-
188 metric Chart of the Oceans) and ETOPO (Earth Topography) bathymetric data.
189 Details on the bathymetry reconstruction are provided in Appendix A.

190 The SLIM model bottom stress is parametrized with a Chézy-Manning drag
191 formulation and a Manning coefficient $n = 0.025 \text{ m}^{-1/3}\text{s}$. The model is forced
192 with wind data from the European Centre for Medium-Range Weather Forecasts
193 (ECMWF) ERA5 reanalysis, which has a spatial resolution of 31 km and a tem-
194 poral resolution of 1 hour. The same wind data is used in OpenOil as well. On

¹SLIM: Second-generation Louvain-la-Neuve Ice-ocean Model, www.slim-ocean.be

195 the open boundary surrounding the SP, we impose a combination of the depth-
196 averaged velocity provided by the Mercator global ocean analysis, produced by
197 running the global data-assimilated ocean model NEMO on a $1/12^\circ$ grid, and the
198 tidal velocity obtained from the OSU TPXO9-atlas dataset (Egbert and Erofeeva,
199 2002). Although the Mercator global ocean analysis accurately reproduces the
200 large-scale ocean circulation patterns in the Indian Ocean, we acknowledge that
201 Vogt-Vincent and Johnson (2023) recently generated multidecadal simulations of
202 the southwestern Indian Ocean with a finer horizontal resolution of $1/50^\circ$. How-
203 ever, these results were not available at the time we conducted this study. More
204 details on the SLIM model formulation can be found in Lambrechts et al. (2008)
205 and Hanert et al. (2023). SLIM has already been used to simulate flows on shal-
206 low submerged platforms or banks similar to SP such as the Great Bahama Bank
207 (Lopez-Gamundi et al., 2022; Purkis et al., 2023) or shallow continental shelf ar-
208 eas such as the Great Barrier Reef (Australia, Lambrechts et al., 2008) and the
209 Florida Reef Tract (Frys et al., 2020). More details on the model validation on the
210 SP are provided in Appendix B.

211 2.3. *Oil spill vulnerability indicators*

212 The backward oil-dispersal simulations generate an ensemble of trajectories
213 originating from receptor points around each sensitive coastal area on the SP and
214 moving backward in time. We follow the approach of Ciappa (2021) to derive
215 vulnerability indicators from the backward oil particles trajectories. By partition-
216 ing the sea surface with a 0.005° (≈ 500 m) resolution grid, we can calculate the
217 number of trajectories intersecting each grid element during each month of the
218 2018-2020 period, as well as the travel time for the oil particles to move from the
219 receptor points to the grid element. Dividing the number of trajectories crossing

220 each grid element during a specific month by the total number of trajectories orig-
221 inating from all the receptor points representing a sensitive coastal area during
222 that time yields a probability map. This map indicates the probability of each grid
223 element being a source of pollution that will reach the coastal area during that
224 month. It can also be interpreted as the fraction of all oil released in that element
225 during the month that would reach the sensitive coastal area.

226 Oil spill risk is formally defined as a combination of the probability of being
227 affected by a spill and the resulting consequences. In this study, we assume that
228 the consequences are comparable for all the selected coastal sites. Therefore, the
229 risk indicator corresponds to the probability of an oil spill released within a 500 m
230 grid element during a specific month reaching a particular coastal site. Monthly
231 risk distribution maps have been averaged over the 2018-2020 period to account
232 for interannual variability in the atmospheric and oceanic circulations on the SP.
233 A time-of-arrival map can also be generated by considering the minimum time
234 required for oil released in a grid element to reach the sensitive coastal area. Both
235 probability and arrival-time maps were calculated for every month of the 2018-
236 2020 period. We then averaged the data for each season (DJF, MAM, JJA, and
237 SON) across the three years to obtain statistically reliable seasonal estimates.

238 Since the most likely source of oil pollution on the SP is currently maritime
239 traffic, either through intentional or accidental releases, we can further refine the
240 oil spill risk maps by combining them with the locations of the main shipping
241 lanes and the most accident-prone areas, which we assume to correspond to ar-
242 eas shallower than 10 m (Fig. 1c). These areas include shallow sandbanks and
243 coral reefs that present a higher risk of ship grounding and subsequent hull dam-
244 age. We also considered offshore areas under oil exploration licence or where

245 oil extraction used to take place (Fig. 1d) as potential sources of pollution. By
246 spatially integrating the oil spill risk distribution over the areas where an oil spill
247 is most likely to occur, either because of shipping or oil extraction activities, we
248 can estimate the total exposure of each sensitive coastal area to both sources of oil
249 pollution and assess how this exposure varies during the year.

250 **3. Results**

251 Oil dispersal across the SP is primarily influenced by the residual ocean cir-
252 culation and wind patterns. The ocean circulation exhibits distinct seasonality in
253 response to the monsoon regime (refer to Appendix C for further details). Conse-
254 quently, oil spills tend to spread more rapidly eastward during the austral summer
255 and westward during the austral winter. To maintain conciseness, we present re-
256 sults for DJF (NW monsoon) and JJA (SE monsoon), as they best represent the
257 seasonal variability observed on the SP. Comprehensive results for all sites and
258 seasons are available as the supplementary online data.

259 *3.1. Arrival time maps*

260 The arrival time maps reveal the minimum duration needed for an oil spill
261 originating from a specific offshore area to reach one of the sensitive coastal lo-
262 cations under study. "Mahé North-West Arrow, Bel Ombre" and "Victoria Port,
263 Saint-Anne Marine Park" (Fig. 2a,a',b,b') are situated on opposite sides of Mahé
264 Island, resulting in different arrival time patterns. The former is more protected
265 from oil spills originating from the east of the plateau, while the latter is better
266 sheltered from spills coming from the western part of the SP. During the DJF
267 season, an oil spill released at the western plateau boundary could reach "Mahé

268 North-West Arrow, Bel Ombre" coasts in under two days (Fig. 2a). In the JJA pe-
269 riod, spills starting at the eastern and southwestern plateau boundaries could reach
270 "Victoria Port, Saint-Anne Marine Park" coasts within one to four days (Fig. 2b').
271 "Silhouette Marine Park" and "Praslin, La Digue, and Curieuse Islands" coasts
272 (Fig. 2c,c',d,d') are geographically exposed from all directions. They face greater
273 exposure to spills from the western side of the plateau during the austral summer
274 and the eastern side during the austral winter. Moreover, an oil spill near Victoria
275 Port, Seychelles' main port, could impact both studied areas within two to four
276 days. Bird and Denis islands display the same general oil dispersal pattern as Sil-
277 houette and Praslin. However, since these islands are situated near the boundaries
278 of the SP, which define the limits of the oil spill dispersal model, a significant por-
279 tion of backtracked oil particles leave the plateau in under one day of simulation
280 (see supplementary data).

281 3.2. *Oil spill risk maps*

282 The probability maps indicate the most likely locations from which an oil spill
283 could impact SP's sensitive coastal areas. Since the consequences of an oil spill
284 can be assumed to be similar for all coastal areas, these probability maps can be
285 interpreted as the oil spill risk faced by the coastal areas. Offshore areas where an
286 oil spill is most likely to occur can be superimposed over the risk maps to better
287 highlight oil spill exposure to both both maritime traffic and oil extraction.

288 Regarding the northwest coast of Mahé and Bel Ombre, the extent of the risk
289 distribution tends to peak during the austral summer (SE monsoon) when north-
290 easterly currents expose these coastal areas to oil spills from the western part of
291 the plateau (Fig. 3a). This exposure diminishes until the austral winter (NW
292 monsoon), when these areas are geographically sheltered from dispersed oil spills

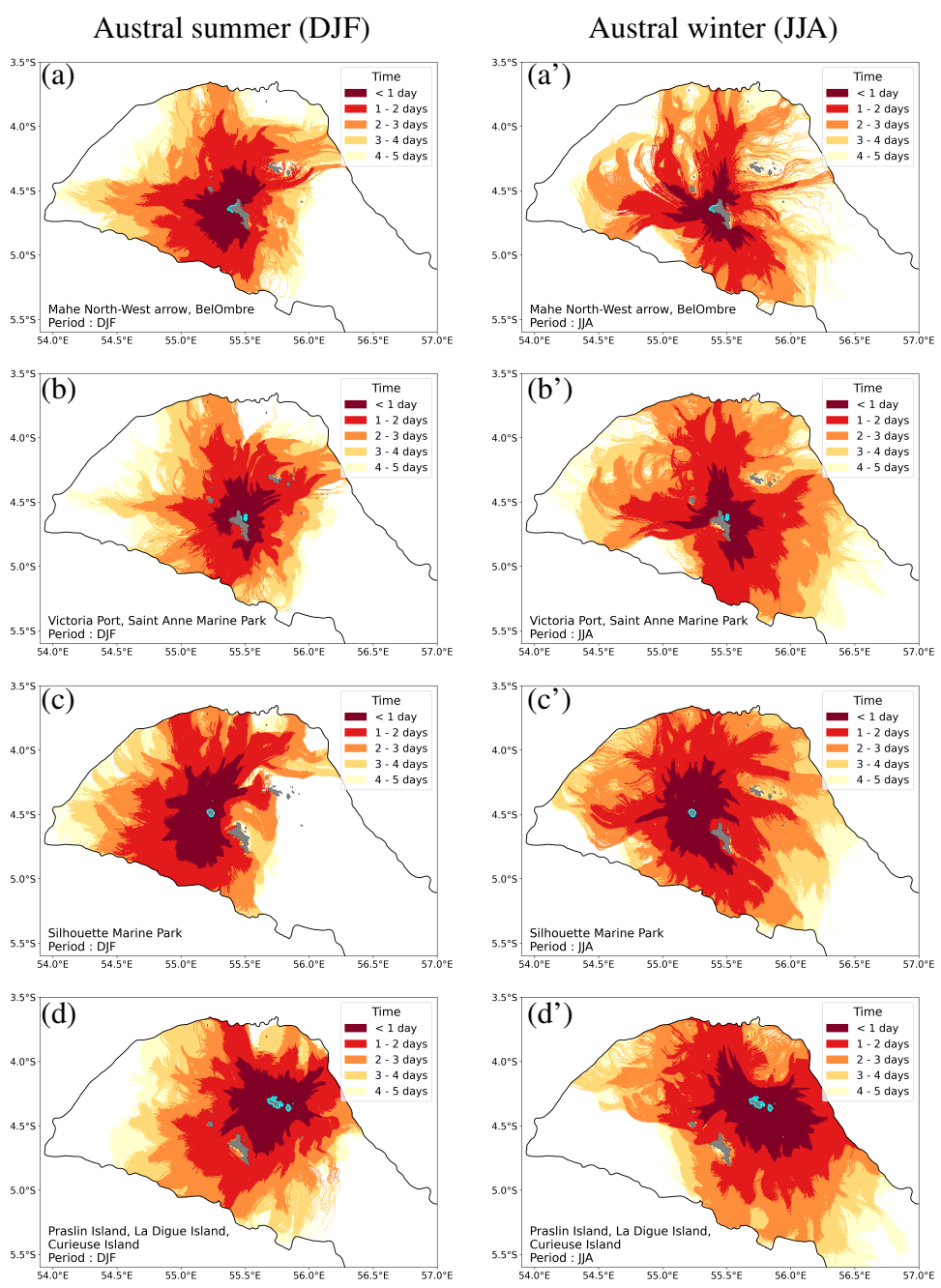


Figure 2: Seasonal variability of the minimum arrival time for an oil spill to reach the (a, a') "Mahé North-West Arrow, Bel Ombre", (b, b') "Victoria Port, Saint-Anne Marine Park", (c, c') "Silhouette Marine Park" and (d, d') "Praslin, La Digue and Curieuse Islands" coastlines. The sensitive coastal areas are highlighted in blue.

293 by south-westerly currents (Fig. 3a'). In this region, oil spill exposure primarily
294 stems from maritime traffic, as the probability area only slightly intersects with
295 oil extraction areas throughout the year.

296 In contrast, Victoria Harbour and St Anne Marine Park, located east of Mahé,
297 are more at risk of being impacted during the austral winter by oil spills originat-
298 ing east of the SP (Fig. 3b'). However, these areas remain more exposed during
299 the austral summer (Fig. 3b) compared to the exposure of the areas on the north-
300 west coast of Mahé during the austral winter (Fig. 3a'). Although these coastal
301 regions appear to have higher exposure to oil exploration areas than the previous
302 ones (especially during the SON season, see suppl. data), they still face greater
303 exposure to shipping routes. During the austral winter, a spill-threatening area can
304 be observed heading north along the major north-south shipping route.

305 The Silhouette Marine Park (Fig. 3c,c') and the islands of Praslin, Curieuse,
306 and La Digue (Fig. 3d,d') are more exposed to oil spills from the west during the
307 austral summer and from the east during the austral winter. Silhouette experiences
308 limited shipping and oil extraction exposure during the first part of the year (DJF
309 and MAM), but this exposure increases during the remainder of the year. Praslin,
310 Curieuse, and La Digue are exposed to both types of exposure throughout the year.
311 Bird Island's coastline appears to have limited exposure to both potential sources
312 of oil spills (Fig. 4a,a'). It is primarily exposed to accidents in the shallow area
313 around the island, which is less than 10 m deep and therefore prone to boat acci-
314 dents. Conversely, Denis Island (Fig. 4b,b') is situated within an oil exploration
315 license area, making it highly susceptible to oil spill risks due to its proximity to
316 oil extraction areas.

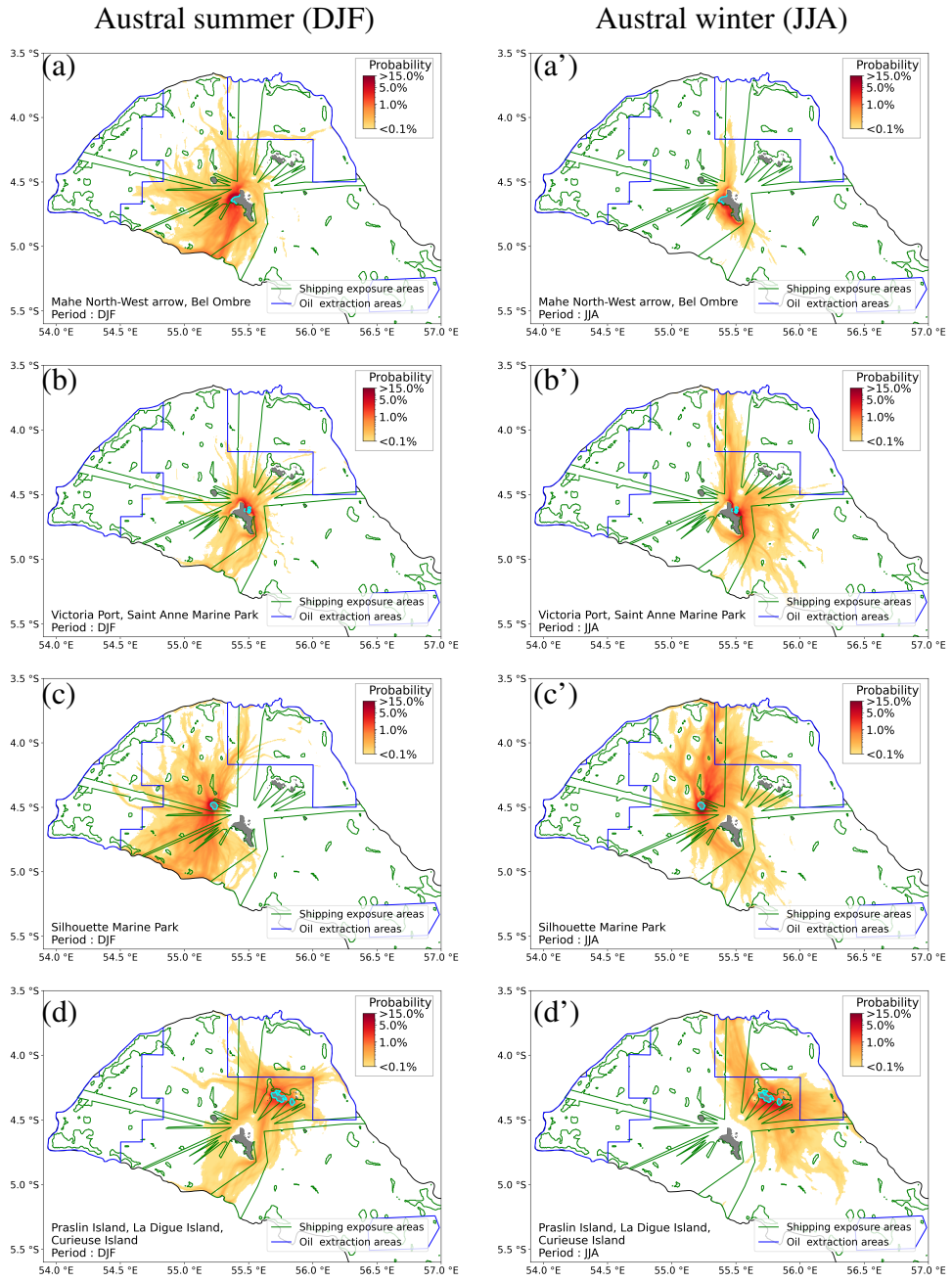


Figure 3: Seasonal variability of the risk distributions for an oil spill to reach the (a,a') "Mahé North-West Arrow, Bel Ombre", (b,b') "Victoria Port, Saint-Anne Marine Park", (c,c') "Silhouette Marine Park" and (d,d') "Praslin, La Digue and Curieuse Islands" coastlines. The sensitive coastal areas are highlighted in blue.

Austral summer (DJF)

Austral winter (JJA)

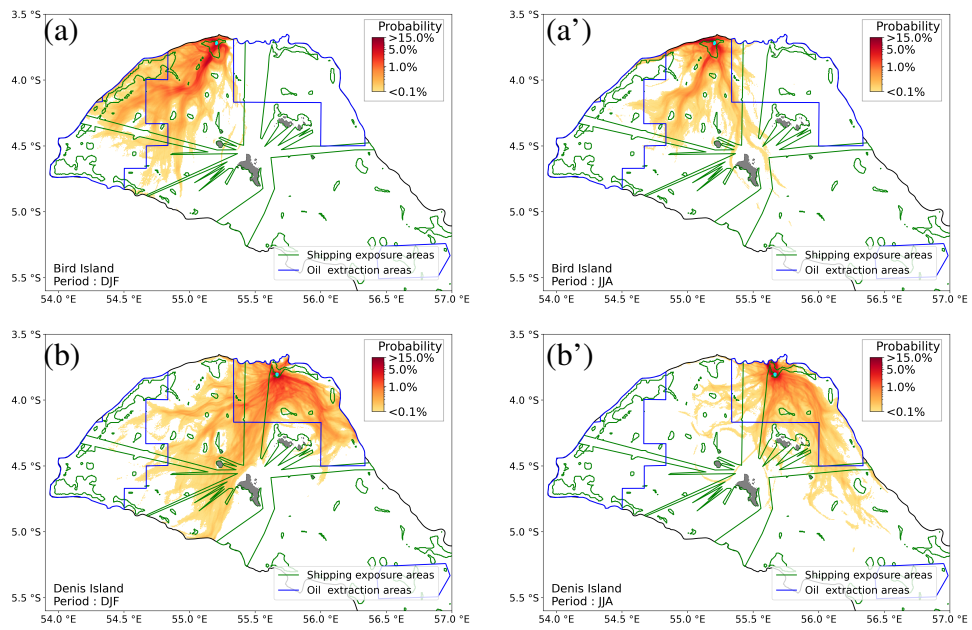


Figure 4: Same as Fig. 3 for (a,a') "Bird Island" and (b,b') "Denis Island" coastlines.

317 *3.3. Total exposure to maritime shipping and oil extraction*

318 The total exposure of each sensitive coastal area to pollution from both ship-
319 ping and oil extraction has been calculated by spatially integrating the oil spill risk
320 patterns over offshore areas with significant shipping traffic (Fig. 1c) and oil ex-
321 traction (Fig. 1d) activities. These exposures to two different sources of pollution
322 have then been monthly averaged over the years 2018-2020 and normalized with
323 respect to the largest monthly value (Fig. 5). Overall, oil extraction pollution pri-
324 marily affects Denis Island (Fig. 5a) since it is located within an oil exploration
325 license area. The other sensitive sites, being farther from oil extraction areas,
326 have considerably lower total exposure, which remains fairly stable throughout
327 the year. The notable exception is Silhouette Marine Park, whose exposure in-
328 creases during the austral spring (SON).

329 Shipping pollution exposure exhibits more variability (Fig. 5b). The total ex-
330 posure time series of the two areas on Mahé Island ("Mahé North-West Arrow, Bel
331 Ombre" and "Victoria Port, Saint-Anne Marine Park") are inversely related. The
332 west coast faces greater vulnerability during the austral summer (DJF), while Vic-
333 toria Harbor and Saint-Anne Marine Park are more vulnerable in the austral winter
334 (JJA). This trend, evident in the risk maps from the previous section, results from
335 the geographical positions of these areas and the change in the atmospheric and
336 oceanic circulation patterns between the two monsoon seasons. The vulnerability
337 of Mahé North-West Arrow and Bel Ombre coasts remains lower than that of Vic-
338 toria Harbor and Saint-Anne Marine Park. This is because the main north-south
339 shipping route passes east of Mahé (to reach Victoria Harbor), hence protecting
340 the western coastal areas from pollution originating from this traffic, particularly
341 during the austral winter.

342 The vulnerability of Silhouette Marine Park and the islands of Praslin, La
343 Digue, and Curieuse to shipping pollution remains relatively constant throughout
344 the year. This is because these areas are exposed from all sides (as all islands
345 coastlines are considered), unlike the areas on Mahé Island, which are geographi-
346 cally protected for part of the year. As for Bird and Denis Islands, these sensitive
347 areas display higher vulnerability during the austral summer and lower vulnerabil-
348 ity during the austral winter. Due to south-westerly currents during this period and
349 the islands' proximity to the plateau boundaries, a large portion of the backtracked
350 oil particles are pushed outside the plateau. Consequently, this vulnerability may
351 be underestimated.

352 **4. Discussion and conclusions**

353 The analysis of six sensitive coastal areas in the Seychelles Plateau (SP) re-
354 veals high vulnerability to oil spills, with strong seasonality driven by atmospheric
355 and oceanic circulations. No part of the plateau can be considered risk-free, and
356 any oil spill incident could potentially impact sensitive coastal areas in less than
357 five days. The main north-south shipping route poses a significant risk to five of
358 the six sensitive coastal areas for at least half of the year.

359 Offshore oil spill risk distributions exhibit considerable seasonal variability as
360 they are influenced by winds, ocean currents, and waves, which change through-
361 out the year. Surface oil particles are directly affected by winds and wind-induced
362 waves, while denser oil particles and those in the water column become less in-
363 fluenced by wind with depth. Wind velocities are high over the SP, particularly
364 during monsoon seasons, significantly impacting oil dispersal. The significant
365 variation in ocean circulation and winds throughout the year results in substan-

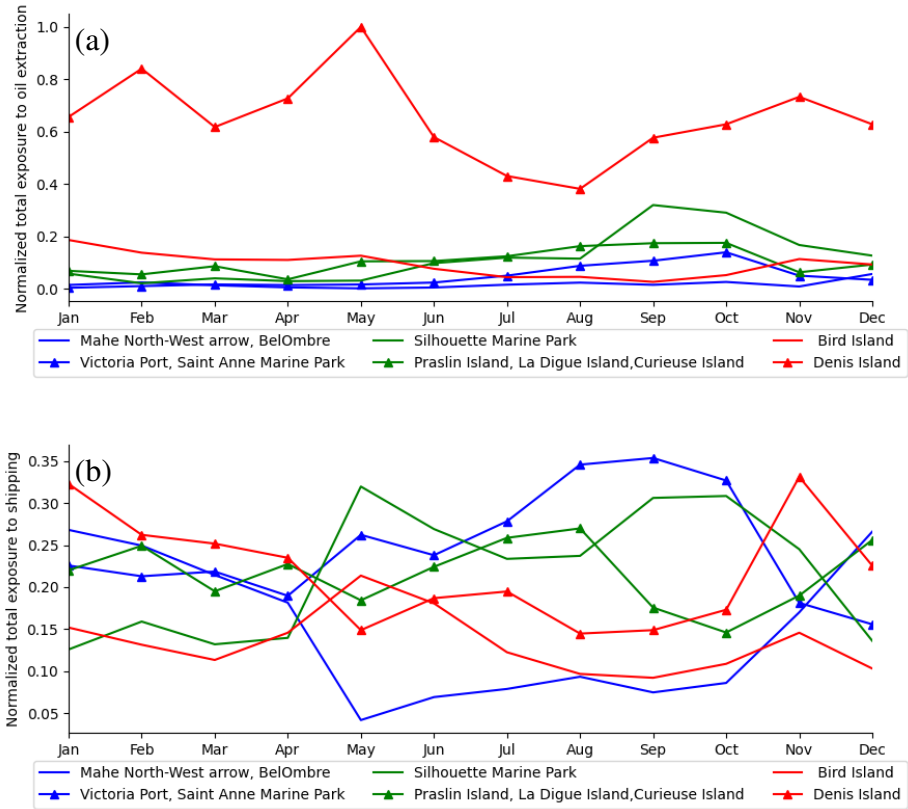


Figure 5: Monthly evolution of total (a) oil extraction and (b) shipping pollution exposure, defined as the spatial integral of the oil spill risk patterns over the offshore areas where those two activities take place, and normalized by the largest monthly value of both indicators.

366 tial changes in the areas threatening SP’s coastlines. The strong seasonal shift
367 in ocean circulation is due to the monsoon system. In a worst-case scenario, an
368 oil spill originating from the northern part of the plateau could reach sensitive
369 coastal areas in less than two days, necessitating an oil spill rapid response plan
370 and efficient infrastructure to combat the spill.

371 Exposure to oil spills from shipping is primarily influenced by a north-south
372 shipping route connecting to the Port of Victoria. Five out of six sensitive coastal
373 areas are vulnerable to potential oil pollution events along this route for at least
374 two seasons of the year. This route is especially threatening as it concentrates
375 most of the shipping activity on the SP. Closely monitoring this route is essential
376 for early detection of spills that could pose significant hazards to numerous coastal
377 assets. Denis Island seems to be the coastal area most vulnerable to potential oil
378 extraction activities, as it is located within one of these areas. However, the actual
379 risk it may pose to Denis Island remains uncertain due to a lack of information
380 regarding the exploration activities in the area, the number of wells that might be
381 exploited in the future and their precise location.

382 Beyond assessing vulnerability to oil spills, this study could also contribute to
383 the assessment of Seychelles coastlines’ vulnerability to other drifting materials
384 that remain relatively close to the ocean surface, and are transported under the
385 combined influence of ocean currents, wind, and waves. The resulting offshore
386 risk distribution is expected to be similar to those derived in this study. This
387 could be the case, for example, with micro and macroplastics settling on coasts, an
388 issue already observed in various locations throughout the Seychelles Archipelago
389 (Dunlop et al., 2020). It could also be the case for jellyfishes, harmful algal blooms
390 and sargassum.

391 This study has however some limitations due to assumptions made or inher-
392 ent in the models used. First, the hydrodynamic simulations are limited by the
393 availability of observational data for validation and heavily depend on the quality
394 of the Mercator global ocean analysis for the external ocean circulation forcing,
395 which might not be optimal (Lellouche et al., 2018). The SLIM model used in
396 the study assumes a vertically homogeneous water column and is hence not suit-
397 able to simulate the circulation beyond the plateau boundaries. The vulnerability
398 assessment could hence only be performed on the plateau and not over the entire
399 Seychelles' EEZ. Furthermore, the study's three-year simulation may not capture
400 the full interannual variability of ocean circulation in the area. To obtain more
401 robust risk estimates, a broader range of simulated years might be necessary. The
402 oil drift simulations are limited to a maximum duration of five days backward-in-
403 time, while weathering processes, such as evaporation and biodegradation, have
404 not been considered. Lastly, limited information about shipping and petroleum
405 extraction poses a significant constraint to the study. Only high shipping density
406 routes have been approximated, with no available spatial distribution of shipping
407 density. For petroleum extraction, aside from areas currently under exploration
408 licenses, there was no data on wells and their spatial distribution made by the
409 company exploring those areas. Access to such information could help refine the
410 study and enable a more quantitative comparison between total exposures to ship-
411 ping and petroleum extraction.

412 Seychelles' oil spill vulnerability is shared by most SIDS. Given this vulner-
413 ability, it is crucial for SIDS to develop an oil spill monitoring and mitigation
414 strategy. This may involve investing in infrastructure and technology to detect
415 and respond to oil spills rapidly, as well as building capacity through training and

416 international collaboration. Given their limited resources, SIDS should prioritize
417 their monitoring resources to the areas from where oil spills would pose the great-
418 est threat to their coastal assets such as those identified here for Seychelles. Fur-
419 thermore, integrating environmental risk assessments into development planning
420 can help these nations better understand their vulnerabilities and adapt accord-
421 ingly. By developing a robust oil spill monitoring and mitigation strategy, SIDS
422 can better protect their unique ecosystems, economies, and communities from the
423 devastating consequences of oil spills. Investing in these measures will enhance
424 the resilience of these islands and ensure their long-term sustainable development.

425 **CRedit authorship contribution statement**

426 **A. Verhofstede:** Software, Investigation, Writing - review & editing. **T.**
427 **Dobbelaere:** Software, Investigation, Writing - review & editing. **J. Harlay:**
428 **Conceptualization, Methodology, Writing - review & editing. E. Hanert:** Con-
429 **ceptualization, Methodology, Writing - original draft, Supervision.**

430 **Declaration of competing interest**

431 The authors declare that they have no known competing financial interests or
432 personal relationships that could have appeared to influence the work reported in
433 this paper.

434 **Data availability**

435 The oil spill arrival time and risk maps for the six selected sites, encompassing
436 all four seasons, can be accessed at [https://doi.org/10.5281/zenodo.](https://doi.org/10.5281/zenodo.8414759)
437 [8414759](https://doi.org/10.5281/zenodo.8414759).

438 **Code availability**

439 The SLIM model source code can be found at <https://git.immc.ucl.ac.be/slim/slim>.

441 **Acknowledgements**

442 Computational resources were provided by the Consortium des Équipements
443 de Calcul Intensif (CÉCI), funded by the F.R.S.-FNRS under Grant No. 2.5020.11.
444 The funders had no role in the study design, data collection and analysis, decision
445 to publish or preparation of the manuscript.

446 **Appendix A. Bathymetry reconstruction on Seychelles Plateau**

447 We examined two bathymetric data sources for the SP: GEBCO (Fig. A.6a)
448 and ETOPO (Fig. A.6b). GEBCO is usually preferred due to its higher resolution
449 of 15 arc seconds compared to ETOPO's 1 arc minute resolution. However, we
450 noted that GEBCO's bathymetric data depict an approximately 700-meter-deep
451 trench in the northeastern part of the plateau (Fig. A.6a). This trench appears
452 unrealistic on a shallow granitic plateau and, to our knowledge, has not been men-
453 tioned in any other studies.

454 To evaluate the accuracy of the GEBCO and ETOPO datasets, we compared
455 them with single-beam bathymetric observations retrieved from the IHO DCDB²,
456 which is hosted by NOAA's National Centers for Environmental Information. Al-
457 though no observations were collected directly in the area where the trench is

²International Hydrographic Organization's Data Centre for Digital Bathymetry, https://www.ncei.noaa.gov/maps/iho_dcdb/

458 located, those obtained in its immediate vicinity suggest that GEBCO is less ac-
459 curate than ETOPO in that region (Fig. A.6c). Nevertheless, observations in
460 other parts of the plateau indicate that GEBCO generally has higher accuracy than
461 ETOPO (Fig. A.6d). Consequently, we decided to merge both datasets, utilizing
462 ETOPO only in the region where the trench is situated and GEBCO for the rest of
463 the plateau. The resulting bathymetry employed in the model is illustrated in Fig.
464 A.7.

465 **Appendix B. Hydrodynamic model validation**

466 Although the hydrodynamic simulations span three years, the model has only
467 been validated for 2018, as more observational data was available for that year.
468 We validated the sea surface elevation using observations from a tide gauge situ-
469 ated north of Mahé island (WSL-925-Seychelles-Pt, 4.5°S, 55.5°E) , provided by
470 the European Commission Joint Research Center’s Space, Security, and Migra-
471 tion directorate, and the current velocities with Acoustic Doppler Current Profiler
472 (ADCP) data from the Seychelles Local Ocean Modeling and Observation pro-
473 gram (SLOMO), collected east of Mahé (Castillo-Trujillo et al., 2021, see location
474 in Fig. 1b). The model accurately reproduces the tidal signal observed in the sea
475 surface elevation time series (Fig. B.8). The root mean square error between the
476 observed and simulated elevation over the entire year of 2018 is 7.5 cm.

477 ADCP velocity measurements east of Mahé suggest that the velocity field is
478 relatively uniform in the vertical direction (Fig. B.9), which justifies the use of a
479 2D depth-averaged model for simulating oil dispersal over the SP. The simulated
480 current velocity amplitude aligns with the observed values, although the model has
481 a tendency to overestimate these values (Figure B.10a). Regarding the direction

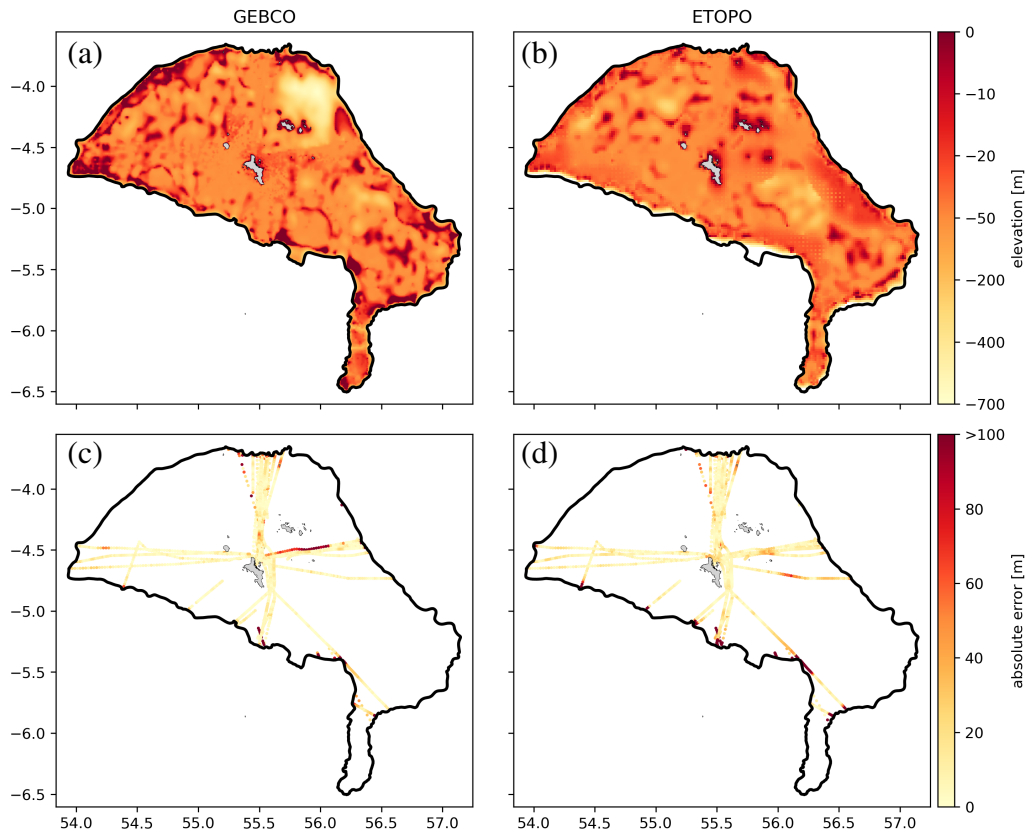


Figure A.6: Comparison between (a) the GEBCO and (b) ETOPO bathymetric data on the SP. The former exhibits a deep trench reaching about -700m in the northeastern part of the plateau that is not present in the latter. Both bathymetric data are compared with bathymetric single beam observations (c-d).

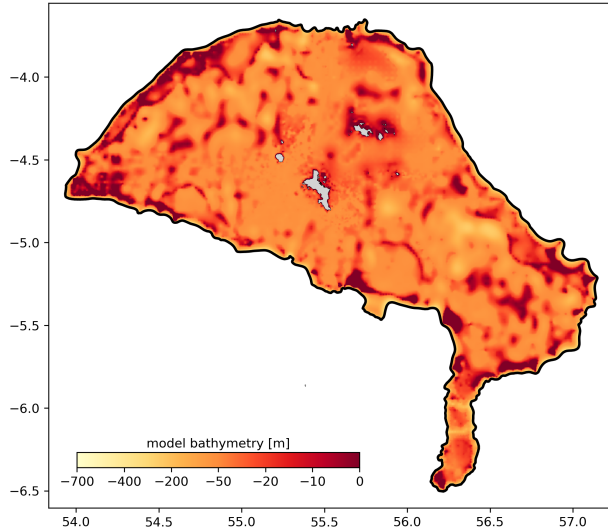


Figure A.7: Bathymetry used in the hydrodynamic model of SP. It has been obtained by merging the GEBCO and ETOPO bathymetric data.

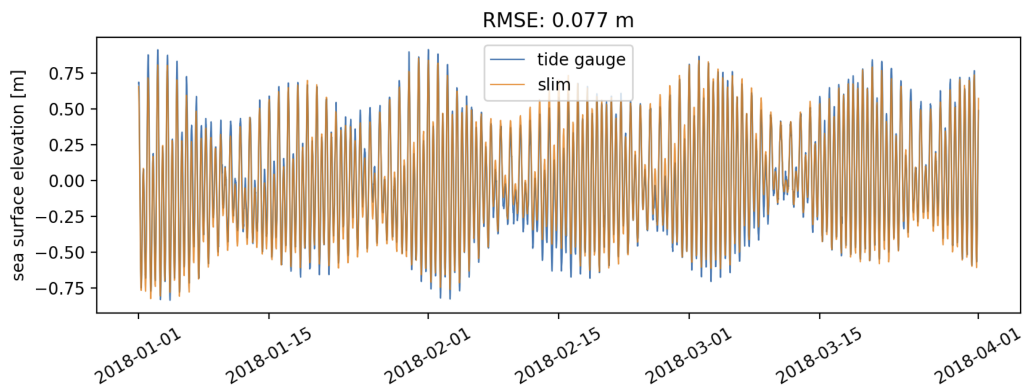


Figure B.8: Comparison of the observed and simulated sea surface elevation. The mean value of the time series was subtracted from all measures to obtain a signal with a zero mean in both cases.

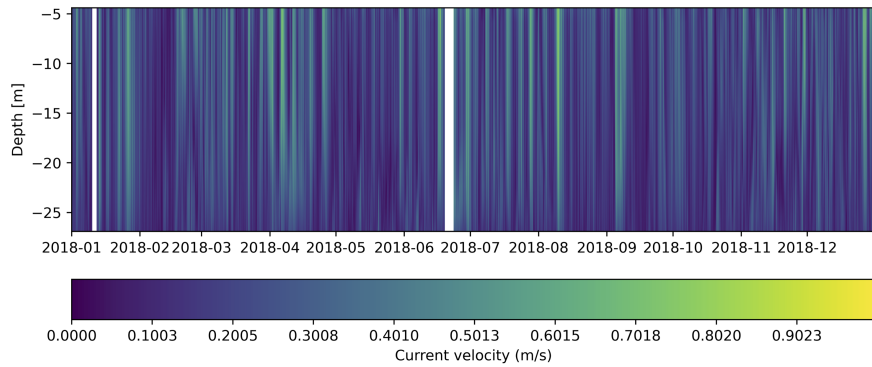


Figure B.9: Current velocity profile recorded by the SLOMO ADCP situated east of Mahé throughout 2018.

482 of the currents, the simulation often predicts more northward currents than those
 483 observed by the SLOMO ADCP (Fig. B.10b).

484 **Appendix C. Seasonal circulation patterns over Seychelles' Plateau**

485 The ocean circulation over the SP is influenced by two monsoon seasons: the
 486 southeast monsoon during the austral winter (June to September), characterized by
 487 northwesterly winds, and the northwest monsoon during the austral summer (De-
 488 cember to March), marked by southeasterly winds. In between these two monsoon
 489 seasons, the winds tend to be weaker and more variable (Castillo-Trujillo et al.,
 490 2021; Schott and McCreary, 2001). The SLIM model simulates northeasterly cur-
 491 rents during the northwest monsoon, with peak current velocities ranging between
 492 0.6 and 0.8 m/s, and southwesterly currents during the southeast monsoon, with
 493 velocities up to 0.5 m/s (Figure C.11). During the inter-monsoon seasons, the cur-
 494 rents are generally weaker and more variable than during the monsoon seasons.

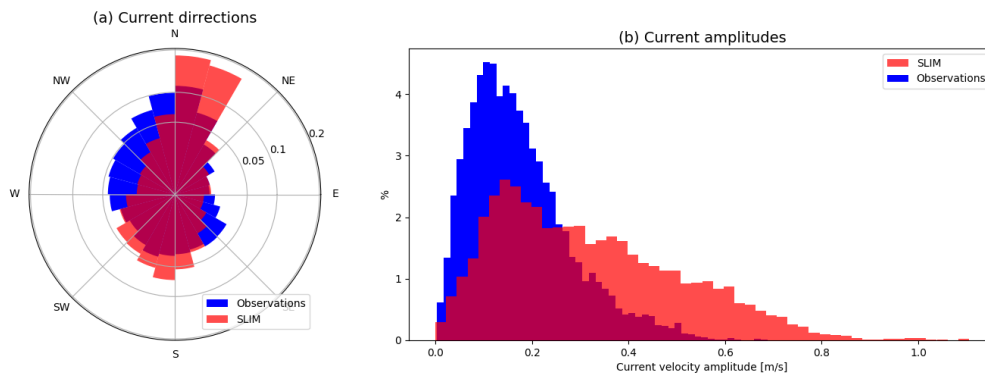


Figure B.10: Comparison of observed and simulated currents in terms of (a) current direction and (b) current amplitude for the entire year of 2018.

495 References

- 496 Agence Française de Développement, 2018. Port of Victoria: A crucial renovation
 497 for the Seychelles. URL: [https://www.afd.fr/en/actualites/
 498 port-victoria-crucial-renovation-seychelles](https://www.afd.fr/en/actualites/port-victoria-crucial-renovation-seychelles).
- 499 Anselain, T., Heggy, E., Dobbelaere, T., Hanert, E., 2023. Qatar peninsula’s vul-
 500 nerability to oil spills and its implications for the global gas supply. *Nature
 501 Sustainability* 6, 273–283. doi:10.1038/s41893-022-01037-w.
- 502 Arduin, F., Marié, L., Rasclé, N., Forget, P., Roland, A., 2009. Observation and
 503 estimation of Lagrangian, Stokes, and Eulerian currents induced by wind and
 504 waves at the sea surface. *Journal of Physical Oceanography* 39, 2820–2838.
- 505 Batchelder, H.P., 2006. Forward-in-time-/backward-in-time-trajectory
 506 (FITT/BITT) modeling of particles and organisms in the coastal ocean.
 507 *Journal of Atmospheric and Oceanic Technology* 23, 727–741.

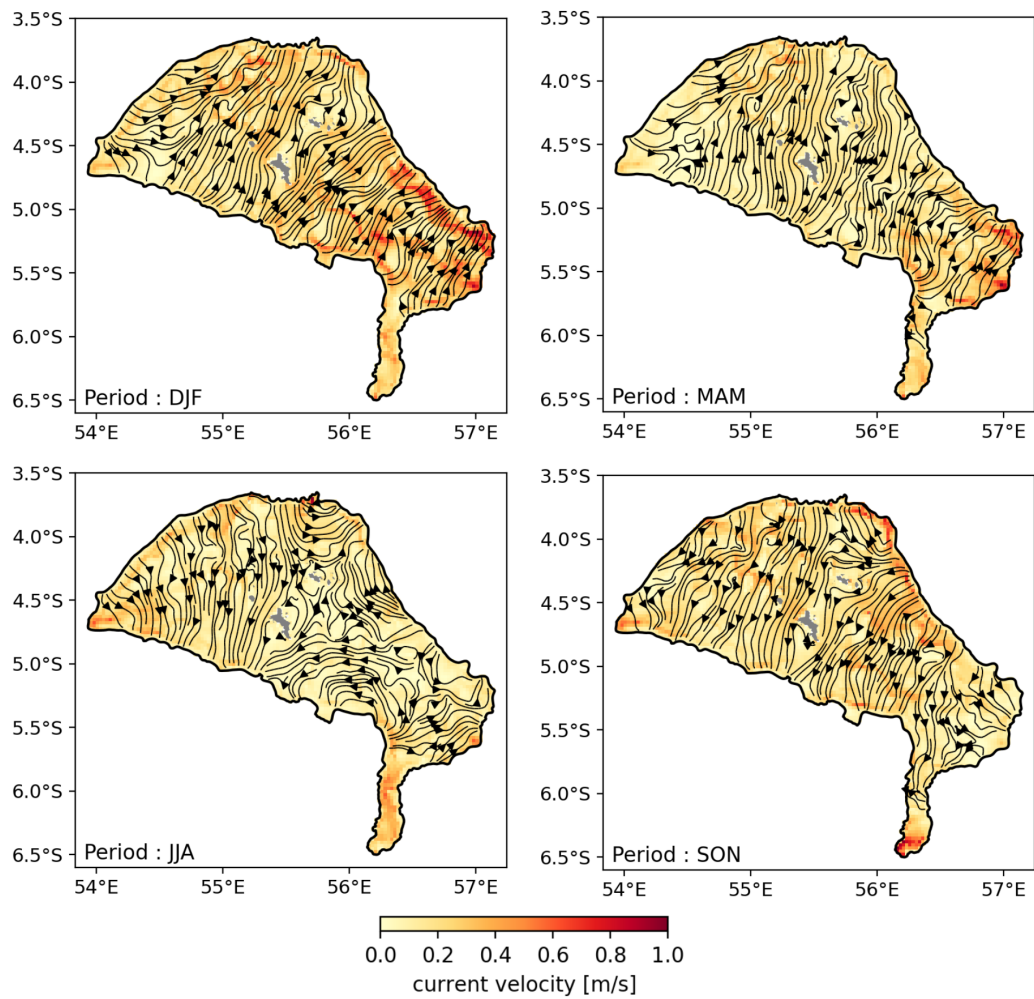


Figure C.11: Seasonal variations in the simulated residual ocean circulation over the Seychelles Plateau, as averaged seasonally from 2018 to 2020.

- 508 Betzold, C., 2015. Adapting to climate change in small island developing states.
509 Climatic Change 133, 481–489.
- 510 Breivik, Ø., Bidlot, J.R., Janssen, P.A.E.M., 2016. A Stokes drift approximation
511 based on the Phillips spectrum. Ocean Modelling 100, 49–56.
- 512 Briguglio, L., 1995. Small island developing states and their economic vulnera-
513 bilities. World Development 23, 1615–1632.
- 514 Campbell, J., Barnett, J., 2010. Climate Change and Small Island States: Power,
515 Knowledge and the South Pacific. Routledge.
- 516 Campling, L., Rosalie, M., 2006. Sustaining social development in a small island
517 developing state? The case of Seychelles. Sustainable Development 14, 115–
518 125.
- 519 Castillo-Trujillo, A.C., Arzeno-Soltero, I.B., Giddings, S.N., Pawlak, G., Mc-
520 Clean, J., Rainville, L., 2021. Observations and modeling of ocean circulation
521 in the Seychelles plateau region. Journal of Geophysical Research: Oceans 126,
522 e2020JC016593.
- 523 Ciappa, A.C., 2021. Reverse trajectory study of oil spill risk in Cyclades Islands
524 of the Aegean Sea. Regional Studies in Marine Science 41, 101580.
- 525 Dagestad, K.F., Röhrs, J., Breivik, Ø., Ådlandsvik, B., 2017. Open-
526 drift v1.0: a generic framework for trajectory modeling. Geoscientific
527 Model Development Discussions URL: <https://gmd.copernicus.org/preprints/gmd-2017-205/gmd-2017-205.pdf>,
528 doi:10.5194/gmd-2017-205,
529 doi:10.5194/gmd-2017-205.

- 530 Dunlop, S.W., Dunlop, B.J., Brown, M., 2020. Plastic pollution in paradise: Daily
531 accumulation rates of marine litter on Cousine Island, Seychelles. *Marine Pol-
532 lution Bulletin* 151, 110803.
- 533 Egbert, G.D., Erofeeva, S.Y., 2002. Efficient inverse modeling of barotropic ocean
534 tides. *Journal of Atmospheric and Oceanic Technology* 19, 183–204.
- 535 Farbotko, C., Lazrus, H., 2012. The first climate refugees? Contesting global
536 narratives of climate change in Tuvalu. *Global Environmental Change* 22, 382–
537 390.
- 538 Frys, C., Saint-Amand, A., Le Hénaff, M., Figueiredo, J., Kuba, A., Walker, B.,
539 Lambrechts, J., Vallaey, V., Vincent, D., Hanert, E., 2020. Fine-scale coral
540 connectivity pathways in the Florida Reef Tract: Implications for conservation
541 and restoration. *Frontiers in Marine Science* 7, 312.
- 542 Government of Seychelles, 2018. Seychelles National Oil Spill Contingency Plan.
543 Technical Report. URL: <https://www.env.gov.sc/downloads>.
- 544 Gurumoorthi, K., Suneel, V., Rao, V.T., Thomas, A.P., Alex, M., 2021. Fate
545 of MV Wakashio oil spill off Mauritius coast through modelling and remote
546 sensing observations. *Marine Pollution Bulletin* 172, 112892.
- 547 Hanert, E., Mohammed, A.V., Veerasingam, S., Dobbelaere, T., Vallaey, V.,
548 Vethamony, P., 2023. A multiscale ocean modelling system for the central
549 Arabian/Persian Gulf: From regional to structure scale circulation patterns. *Es-
550 tuarine, Coastal and Shelf Science* 282, 108230.
- 551 ITOPF, 2005. Seychelles - Country & Territory Profile. URL:

552 [`https://www.itopf.org/fileadmin/uploads/itopf/data/`](https://www.itopf.org/fileadmin/uploads/itopf/data/)
553 `Documents/Country_Profiles/seychell.pdf`.

554 Jones, C.E., et al., 2016. Measurement and modeling of oil slick transport: Mea-
555 surement and modeling oil slick transport. *Journal of Geophysical Research:*
556 *Oceans* 121, 7759–7775.

557 Lambrechts, J., Hanert, E., Deleersnijder, E., Bernard, P.E., Legat, V., Remacle,
558 J.F., Wolanski, E., 2008. A multi-scale model of the hydrodynamics of the
559 whole Great Barrier Reef. *Estuarine, Coastal and Shelf Science* 79, 143–151.

560 Lellouche, J.M., Greiner, E., Le Galloudec, O., Garric, G., Regnier, C., Drevillon,
561 M., Benkiran, M., Testut, C.E., Bourdalle-Badie, R., Gasparin, F., Hernandez,
562 O., Levier, B., Drillet, Y., Remy, E., Le Traon, P.Y., 2018. Recent updates to the
563 Copernicus Marine Service global ocean monitoring and forecasting real-time
564 1/12° high-resolution system. *Ocean Science* 14, 1093–1126.

565 Lopez-Gamundi, C., Dobbelaere, T., Hanert, E., Harris, P.M., Eberli, G., Purkis,
566 S.J., 2022. Simulating sedimentation on the Great Bahama Bank - Sources,
567 sinks and storms. *Sedimentology* 69, 2693–2714.

568 MarineTraffic, 2023. MarineTraffic: Shipping density map over Seychelles
569 plateau in 2021. URL: [`https://www.marinetraffic.com/en/ais/`](https://www.marinetraffic.com/en/ais/home/centerx:55.3/centery:-4.6/zoom:8)
570 `home/centerx:55.3/centery:-4.6/zoom:8`.

571 McEwen, D., Bennett, O., 2010. Seychelles tourism value chain analy-
572 sis. Study for STB commissioned by the Commonwealth Secretariat 76.
573 URL: [`https://www2.gwu.edu/~iits/unwto2012/Seychelles_`](https://www2.gwu.edu/~iits/unwto2012/Seychelles_Tourism_Value_Chain.pdf)
574 `Tourism_Value_Chain.pdf`.

- 575 Nurse, L.A., McLean, R.F., Agard, J., Briguglio, L.P., Duvat-Magnan, V., Pele-
576 sikoti, N., Tompkins, E., Webb, R., 2014. Small islands, in: *Climate Change*
577 *2014: Impacts, Adaptation, and Vulnerability. Part B: Regional Aspects. Con-*
578 *tribution of Working Group II to the Fifth Assessment Report of the Intergov-*
579 *ernmental Panel on Climate Change.* Cambridge University Press, pp. 1613–
580 1654.
- 581 PetroSeychelles, 2023. Blocks licensing - current active licences. URL: [http://petroseychelles.com/index.php/blocks-licensing/
582 //petroseychelles.com/index.php/blocks-licensing/
583 currently-active-licenses.](http://petroseychelles.com/index.php/blocks-licensing/currently-active-licenses)
- 584 Podhorodecka, K., 2018. The economic significance of the tourism sector in Sey-
585 chelles in the wake of global economic crisis. *Economic Problems of Tourism*
586 *43*, 29–40.
- 587 Purkis, S.J., Oehlert, A.M., Dobbelaere, T., Hanert, E., Harris, P., 2023. Always a
588 white Christmas in the Bahamas: temperature and hydrodynamics localize win-
589 ter mud production on Great Bahama Bank. *Journal of Sedimentary Research*
590 *93*, 145–160.
- 591 Rocamora, G.J., Skerrett, A., 2001. *Seychelles.* Pisces Publications and BirdLife
592 International. pp. 751–768.
- 593 Röhrs, J., Dagestad, K.F., Asbjørnsen, H., Nordam, T., Skancke, J., Jones, C.E.,
594 Brekke, C., 2018. The effect of vertical mixing on the horizontal drift of oil
595 spills. *Ocean Science* *14*, 1581–1601.
- 596 Scheyvens, R., Momsen, J.H., 2008. Tourism in small island states: From vulner-
597 ability to strengths. *Journal of Sustainable Tourism* *16*, 491–510.

598 Schott, F.A., McCreary, J.P., 2001. The monsoon circulation of the Indian Ocean.
599 Progress in Oceanography 51, 1–123.

600 Seychelles Fishing Authority, 2019. Mahé plateau trap and line fishery
601 co-management plan. URL: [https://sfa.sc/images/2021/06/](https://sfa.sc/images/2021/06/18/Mahe_Plateau_Trap_and_Line_Fishery_Co-Mangement_Plan_-_March_2019.pdf)
602 18/Mahe_Plateau_Trap_and_Line_Fishery_Co-Mangement_
603 Plan_-_March_2019.pdf.

604 Techera, E.J., 2019. Protected area law in Seychelles: Legal complexity in a
605 micro-jurisdiction. The International Journal of Marine and Coastal Law 34,
606 698–730.

607 The New York Times, 1970. Tanker Goes Down Off the Seychelles; Oil Threatens
608 Isles. URL: [https://www.nytimes.com/1970/06/02/archives/](https://www.nytimes.com/1970/06/02/archives/article-1-no-title.html)
609 article-1-no-title.html.

610 Tkalich, P., Chan, E.S., 2002. Vertical mixing of oil droplets by breaking waves.
611 Marine Pollution Bulletin 44, 1219–1229.

612 Vogt-Vincent, N.S., Johnson, H.L., 2023. Multidecadal and climatological sur-
613 face current simulations for the southwestern Indian Ocean at 1/50° resolution.
614 Geoscientific Model Development 16, 1163–1178.

615 World Travel & Tourism Council, 2022. Seychelles - 2022 Annual Research: Key
616 Highlights. Technical Report. URL: [https://wttc.org/research/](https://wttc.org/research/economic-impact)
617 economic-impact.

618 Zabasajja, J., Bhuckory, K., 2022. Shrinking Seychelles seeks
619 to leverage oil to grow clean power. URL: <https://>

620 www.bloomberg.com/news/articles/2022-11-09/
621 [-shrinking-seychelles-seeks-to-leverage-oil-to-grow-clean-power.](#)

622 Zodiatis, G., et al., 2016. The Mediterranean decision support system for marine
623 safety dedicated to oil slicks predictions. *Deep Sea Research Part II: Topical*
624 *Studies in Oceanography* 133, 4–20.